ELSEVIER

Journal of Nuclear Materials 283–287 (2000) 435–439

journal of nuclear materials

www.elsevier.nl/locate/jnucmat

Tensile properties and damage microstructures in ORR/HFIR-irradiated austenitic stainless steels

E. Wakai [a,*], N. Hashimoto [b], J.P. Robertson [b], S. Jistukawa [a], T. Sawai [a], A. Hishinuma [a]

[a] *Japan Atomic Energy Research Institute, Tokai, Ibaraki, 319-1195, Japan*
[b] *Oak Ridge National Laboratory, P.O. Box 2008, Oak Ridge, TN 37831-6376, USA*

Abstract

The synergistic effect of displacement damage and helium generation under neutron irradiation on tensile behavior and microstructures of austenitic stainless steels was investigated. The steels were irradiated at 400°C in the spectrally-tailored (ST) Oak Ridge research reactor/high flux isotope reactor (ORR/HFIR) capsule to 17 dpa with a helium production of about 200 appm and in the HFIR target capsule to 21 and 34 dpa with 1590 and 2500 appm He, respectively. The increase of yield strength in the target irradiation was larger than that in the ST irradiation because of the high-number density of Frank loops, bubbles, voids, and carbides. Based on the theory of dispersed barrier hardening, the strengths evaluated from these clusters coincide with the measured increase of yield strengths. This analysis suggests that the main factors of radiation hardening in the ST and the target irradiation at 400°C are Frank-type loops and cavities, respectively. © 2000 Elsevier Science B.V. All rights reserved.

1. Introduction

One of the favored first wall and blanket concepts for near term fusion systems such as the international thermonuclear experimental reactor (ITER) is a low-pressure water-cooled type of austenitic stainless steel [1] and reduced-activation ferritic steel structure. In the D–T fusion reactor, the neutrons, with a maximum energy of 14 MeV, create displacement damage in the first-wall materials, and also produce hydrogen and helium atoms from (n, p) and (n, α) reactions. The accommodation of these gas atoms generated in these steels during irradiation may induce radiation-embrittlement, such as the degradation of fracture toughness and elongation. In this study, the changes in tensile properties and microstructures of austenitic stainless steels induced by irradiation were examined to understand the synergistic effect of displacement damage and helium generation under the simulated fusion neutron environment. This experiment was conducted under the DOE/JAERI collaborative agreement.

2. Experimental procedure

The spectrally tailored (ST) experiments [2–7] were performed in two stages. The first stage of the irradiation was carried out in the Oak Ridge research reactor (ORR) in the capsule ORR-MFE-7J, which operated at 400°C. In the ORR capsule, water filled the reactor core-piece to 5.9 dpa, and after that it was replaced with solid aluminum to 7.4 dpa. After accumulating approximately 7.4 dpa in the ORR, the specimens were transferred to the high flux isotope reactor (HFIR) in the capsule HFIR-RB-400J-1, which also operated at 400°C to 17.3 dpa. The HFIR capsule was surrounded by a 4.2 mm thick hafnium shield in order to reduce the thermal-neutron flux and maintain a He/dpa level near that expected in a fusion reactor. Temperatures were continuously measured and controlled in these experiments during these irradiation. In

* Corresponding author. Present address: Department of Materials Science, Japan Atomic Energy Research Institute, Tokai Research Establishment, Tokai, Ibaraki-ken 319-1195, Japan. Tel.: +81-29 282 6563; fax: +81-29 282 5922.

E-mail address: wakai@realab01.tokai.jaeri.go.jp (E. Wakai).

0022-3115/00/$ - see front matter © 2000 Elsevier Science B.V. All rights reserved.
PII: S0022-3115(00)00082-9

addition to the ST experiment, irradiations were performed in the HFIR target region at 400°C in capsules designed JP-1, JP-2 and JP-3. The details of neutron fluences and damage levels are given in Table 1.

Chemical compositions of the JPCA and J316 alloys in this study and the heat treatments are given in Table 2. The JPCA steel contains boron, phosphorus, and titanium. The J316 is a standard type 316 stainless steel. The JPCA and J316 alloys were solution annealed (SA) before irradiation. Tensile tests were conducted at the irradiation temperatures in a vacuum of about 1×10^{-3} Pa at strain rates of 4.2×10^{-4} to 5.6×10^{-4} s^{-1}. The tensile specimens were either rod type with gauge sections 18.3 mm long and 2.03 mm in diameter, or SS-1 flat type with gage section 20.32 mm long, 1.52 mm wide, and 0.76 mm thick. The microstructures of these alloys were examined using a JEM-2000FX transmission electron microscope with a LaB_6 gun operated at 200 kV. In order to evaluate defect density, the foil thickness of each TEM specimen was measured by thickness fringes or by the improved CSS method [8,9].

3. Results

The dependence of tensile properties of JPCA-SA steels irradiated at 400°C on the displacement damage under the ST ORR/HFIR and the HFIR target irradiation is given in Table 3 and graphically shown in Fig. 1. The 0.2% offset yield and ultimate tensile strengths in the JPCA-SA steels are plotted against the displacement damage, as shown in Fig. 1(a). These strengths increased rapidly during the first-damage increment, but the increase was less with each succeeding increment. The increase in the strength in the HFIR target irradiation was considerably larger than that in the ST experiment. The uniform and total elongations in the JPCA-SA steels are also plotted against damage, as given in Fig. 1(b). The uniform elongations in the steels decreased significantly with irradiation, and they were only several percent and less than 1%, respectively, for the ST ORR/HFIR and the HFIR target irradiation. The total elongations for these irradiations were nearly equal and at 4–8%. The dependence of tensile properties of J316-SA steels irradiated at 400°C under the ST irradiation was very similar to that in the JPCA-SA steels, as given in Table 3.

Frank-type dislocation loops, carbides and cavities were formed in the JPCA-SA and J316-SA steels during these irradiation at 400°C, as shown in Fig. 2. The number densities and sizes for these defect clusters are given in Table 4. The number densities of dislocation loops and carbides in the HFIR target irradiation were about twice those in the ST ORR/HFIR irradiation. The number density of cavities in the HFIR target irradiation was one order of magnitude higher than that in the ST one. The mean sizes of dislocation loops and voids in the former were smaller than those in the latter irradiation. The mean sizes of carbides in the JPCA-SA steel

Table 1
Irradiation conditions for JPCA and J316 steels in the ST ORR/HFIR capsules and the HFIR target capsules

Capsule	ST irradiation			HFIR target irradiation		
	ORR-MFE-7J	HFIR-MFE-400J-1	ORR-MFE-7J/HFIR-MFE-400J-1	JP-1	JP-2	JP-3
Neutron energy	*Fluence* ($\times 10^{21}$ n/cm^2)			*Fluence* ($\times 10^{21}$ n/cm^2)		
Total	27.0	33.3	60.3	93.8	160.8	148.0
Thermal (<0.5 eV)	8.1	4.0	12.1	38.4	65.8	60.9
0.5 eV–0.1 MeV	9.5	13.0	22.5	30.3	52.0	47.7
>0.1 MeV	9.5	16.4	25.9	25.1	43.0	39.5
>1 MeV	5.1	5.9	11.0	12.7	21.8	20.2
Damage level, dpa	7.4	9.9	17.3	21	36	34
He level, appm	155 (100[a])	125 (100[a])	280 (200[a])	1585	2817	2501
Specimen type	TEM tensile (SS-1)	TEM tensile (SS-1)	TEM tensile (SS-1)	Tensile (rod)	Tensile (rod)	TEM

[a] Value of He production for J316 steel.

Table 2
Alloy compositions (wt%) and heat treatments[a]

Alloy	Fe	Cr	Ni	B	C	N	P	S	Si	Ti	Mn	Mo
JPCA	Bal.	14.2	15.6	0.003	0.06	0.0039	0.027	0.005	0.50	0.24	1.77	2.3
J316	Bal.	16.8	13.5	–	0.06	–	0.028	0.003	0.61	0.005	1.80	2.5

[a] Heat treatment: JPCA, 1090°C/1 h/AC; J316, 1050°C/1 h/AC.

Table 3
Tensile properties of the JPCA-SA and J316-SA steels tested at 400°C

Alloy	Damage	Irradiation temperature (°C)	YS (MPa)	UTS (MPa)	Eu (%)	Et (%)	Ref.
ST irradiation							
JPCA-SA	0	–	274	492	26.0	28.6	–
JPCA-SA	7	400	505	652	10.5	12.9	–
			549	667	2.5	10.5	–
JPCA-SA	17	400	669	729	3.4	5.8	–
			666	728	3.2	5.2	–
J316-SA	0	–	252	476	26.1	28.4	[6]
			222	476	33.0	35.1	[6]
J316-SA	7	400	595	677	4.6	7.0	[6]
			650	717	4.3	6.8	[6]
J316-SA	17	400	663	720	2.4	4.3	[6]
			634	716	5.8	8.1	[6]
HFIR target irradiation							
JPCA-SA	21	400	902	905	0.4	6.2	[10]
JPCA-SA	36	400	872	899	0.6	5.7	[10]

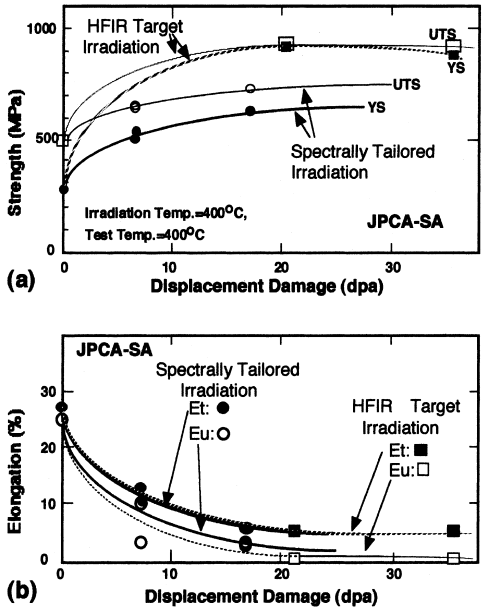

Fig. 1. (a) Yield and ultimate tensile strengths and (b) uniform and total elongations as a function of displacement damage for JPCA-SA steels irradiated at 400°C in the ST ORR/HFIR and the HFIR target capsules.

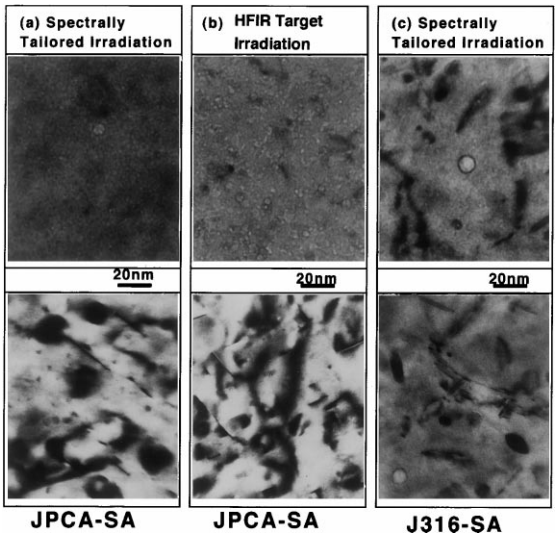

Fig. 2. Microstructures formed at 400°C in: (a) JPCA-SA, (b) J316-SA steels irradiated in the ST ORR/HFIR capsules, and (c) JPCA-SA steel irradiated in the HFIR target capsule.

were similar in each irradiation. The number densities of carbides in the JPCA-SA steel were higher than those in the J316-SA steel under the ST irradiation.

4. Discussion

The effects of He generation on hardening for austenitic steels irradiated in the HFIR and HFR reactors has been reported by Jitsukawa et al. [12], and in the EBR-II and HFIR reactors by Mansur and Grossbeck [13]. In the steels with a high helium production, more-radiation hardening was observed in their examinations of the tensile properties. The detailed reason for the hardening could not be explained, but the cause was thought to be helium atoms in lattice sites and helium bubble formation. Therefore, it is very important to examine in detail the relation between the tensile properties and microstructures.

The model of estimation for the increase of yield strength caused by the radiation-induced micro-clusters is based on Orowan's theory for athermal bowing of

Table 4
Summary of dislocation loops (Frank-type), bubbles, voids, and precipitates formed in the JPCA-SA and J316-SA steels irradiated at 400°C in the ST ORR/HFIR and the HFIR target capsules. The number density and mean size are denoted as N and d, respectively

	Damage (dpa)	Frank-loops N (m^{-3}), d (nm)	Bubbles N (m^{-3}), d (nm)	Voids N (m^{-3}), d (nm)	MC carbides N (m^{-3}), d (nm)	M_6C carbides N (m^{-3}), d (nm)	Ref.
ST irradiation							
JPCA-SA	17	1×10^{21}, 15.7	7×10^{21}, 3.0	8×10^{19}, 9.5	8×10^{21}, 3.4	1×10^{21}, 7.4	Present data
316R-SA	17	1×10^{22}, 20.2	1×10^{22}, 3.0	5×10^{19}, 11.0	2×10^{20}, 7.2	9×10^{20}, 7.1	Present data
HFIR target irradiation							
JPCA-SA	34	2.4×10^{22}, 12.3	2.8×10^{23}, 2.6	1×10^{22}, 5.0	1.4×10^{22}, 3.4	–	[11]

dislocations around obstacles in a slip plane, and this is summarized by Bement [14]. The defects that contribute to the strength in an irradiated steel are given as: Frank-type dislocation loops, black dots, precipitates, cavities (either bubbles or voids), and dislocation network. These defects can be divided into two classes: short-range and long-range obstacles. The short-range obstacles are defined as those which influence moving dislocations only on the same slip plane as opposed to long-range obstacles which impede dislocation motion on slip planes not containing the obstacle [15]. In this model, only the network dislocations are long-range obstacles. The contributions to hardening by short- and long-range obstacles are combined as follows [14]:

$$\Delta\sigma_{YS} = \Delta\sigma_{SR} + \Delta\sigma_{LR}, \tag{1}$$

where $\Delta\sigma_{YS}$, $\Delta\sigma_{SR}$, and $\Delta\sigma_{LR}$ represent the strength estimated from all defect clusters, the short-range obstacles, and the long-range obstacles, respectively.

In this experiment, after 400°C irradiation, the radiation-induced defect clusters observed were Frank-type loops, bubbles, voids, and carbides, and $\Delta\sigma_{YS}$ is therefore described as

$$\Delta\sigma_{YS} = \Delta\sigma_{SR} = \{(\Delta\sigma_{loops})^2 + (\Delta\sigma_{bubbles})^2 + (\Delta\sigma_{voids})^2 + (\Delta\sigma_{precipitates})^2\}^{1/2}, \tag{2}$$

where $\Delta\sigma_{loops}$, $\Delta\sigma_{bubbles}$, $\Delta\sigma_{voids}$, and $\Delta\sigma_{precipitates}$ represent the strength increase estimated from dislocation loops, bubbles, voids, and precipitates, respectively. The contribution from each type of short-range obstacle is described as follows:

$$\Delta\sigma_i = M\alpha\mu b(N_i d_i)^{1/2}, \tag{3}$$

where M, α, μ, b, N_i, and d_i are factors converting critical-resolved shear stress in a single crystal to the uniaxial yield stress in a random crystal, the barrier strength of i-type of obstacle such as dislocation loops, the shear modulus of matrix, the Burger's vector of moving dislocation, the number density of the obstacles, and the mean diameter of the obstacles, respectively. These factor values for austenitic stainless steels have been obtained by several researchers [16–21], and the values are given in Table 5.

From Eq. (2), the contribution of each defect to the total $\Delta\sigma_{YS}$ can be determined as (for example, Frank loops)

$$(\Delta\sigma_{loop})^* = (\Delta\sigma_{loop})^2/\Delta\sigma_{YS}. \tag{4}$$

The increase of strength estimated from these defect clusters in JPCA-SA under the ST irradiation and the HFIR target irradiation are evaluated as 344 and 666 MPa, respectively, and these values coincide with the increase of yield strength obtained from the tensile tests (Fig. 3). For the J316-SA under the ST irradiation, the value is calculated as 406 MPa, and it also coincides with the experimental data. In the ST irradiation, Frank-type

Table 5
The values of the M factor, barrier strength of obstacles, the shear modulus of matrix, the Burger's vector of moving dislocation in austenitic stainless steels

	M	α (Frank-type)	α (bubbles)	α (voids)	α (small carbides)	μ	b
	3.06	~0.45	0.2	~1	~0.4	~70 GMPa (at 400°C)	2.55×10^{-10} m
Ref.	[16]	[17–19]	[20]	[17]	[18]	[21]	

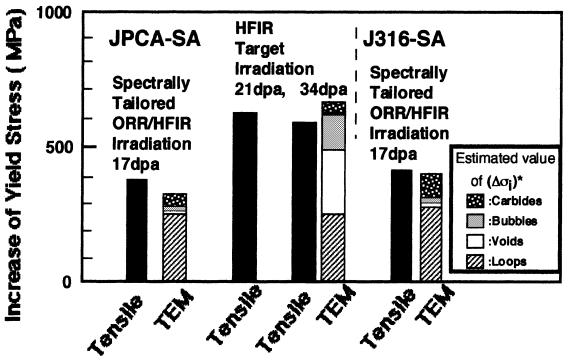

Fig. 3. Comparison of increase of yield strength obtained from tensile tests and the values evaluated from the microstructures in the JPCA-SA and J316-SA steels irradiated at 400°C in the ST ORR/HFIR and the HFIR target capsules.

loops are the main contributor to the increase in yield strength, and in the HFIR target irradiation, cavities are largely responsible for the increment of the strength as shown in Fig. 3. The strength component $(\Delta\sigma_i)^*$ for each obstacle can be seen in the figure. The good correlation between the model and the experimental data shows that the equations and values used in this study are appropriate.

5. Conclusions

The changes in tensile properties and microstructures of SA austenitic stainless steels induced by irradiations in the ST ORR/HFIR capsule and in the HFIR target have been examined to understand the synergistic effect of displacement damage and helium generation under the fusion neutron environment. This study, based on the theory of dispersed barrier hardening suggests that the main factors of hardening in the ST ORR/HFIR and the HFIR target irradiation are Frank-type loops and cavities, respectively.

Acknowledgements

The authors would like to thank Drs A.F. Rowcliffe and S.J. Zinkle in Oak Ridge National Laboratory for their fruitful discussions. We are also grateful to Messrs L.T. Gibson, J.W. Jones, J.J. Duff and the members of the irradiated materials examination and testing laboratory of ORNL for the technical support.

References

[1] G.L. Kulcinski, J. Nucl. Mater. 122&123 (1984) 457.
[2] F. Rowcliffe, A. Hishinuma, M.L. Grossbeck, S. Jitsukawa, J. Nucl. Mater. 179–181 (1991) 125.
[3] R.E. Stoller, P.J. Maziasz, A.F. Rowcliffe, M.P. Tanaka, J. Nucl. Mater. 155–157 (1988) 1328.
[4] T. Sawai, P.J. Maziasz, H. Kanazawa, A. Hishinuma, Fusion Reactor Materials Semiannual Progress Report for Period Ending 30 September 1990, Office of Fusion Energy, DOE/ER-0313/9, 1990, p. 152.
[5] T. Sawai, P.J. Maziasz, H. Kanazawa, A. Hishinuma, J. Nucl. Mater. 191–194 (1992) 712.
[6] J.P. Robertson, I. Ioka, A.F. Rowcliffe, M.L. Grossbeck, S. Jitsukawa, in: R.K. Nanstad, et al. (Eds.), Proceedings of the 18th International Symposium, ASTM STP 1325, American Society for Testing and Materials, Philadelphia, PA, 1997.
[7] N. Hashimoto, E. Wakai, J.P. Robertson, T. Sawai, A. Hishinuma, J. Nucl. Mater. 280 (2000) 186.
[8] T. Sawai, M. Suzuki, P.J. Maziasz, A. Hishinuma, J. Nucl. Mater. 187 (1992) 146.
[9] T. Sawai, M. Suzuki, Scr. Metall. 24 (1990) 2047.
[10] S. Jitsukawa, M.L. Grossbeck, A. Hishinuma, J. Nucl. Mater. 191–194 (1992) 790.
[11] M.P. Tanaka, S. Hamada, A. Hishinuma, P.J. Maziasz, J. Nucl. Mater. 155–157 (1988) 801.
[12] S. Jitsukawa, M.L. Grossbeck, A. Hishinuma, J. Nucl. Mater. 191–194 (1992) 790.
[13] L.K. Mansur, M.L. Grossbeck, J. Nucl. Mater. 155–157 (1988) 130.
[14] A.L. Bement, Jr., in: Proceedings of the Second International Conference on Strength of Metals and Alloys, ASM Metals Park, OH, 1970, p. 693.
[15] R.L. Simons, L.A. Hubert, in: F.A. Garner, J.S. Perrin (Eds.), Effects of Radiation on Materials, vol. II, ASTM, Philadelphia, PA, 1985, p. 820.
[16] R.E. Roger, S.J. Zinkle, in: Proceedings of the Ninth International Conference on Fusion Reactor Materials, Colorado Springs, USA, 1999.
[17] F. Garner, M. Hamilton, N. Panayotou, G. Johnson, J. Nucl. Mater. 103&104 (1981) 803.
[18] M.L. Grossbeck, P.J. Maziasz, A.F. Rowcliffe, J. Nucl. Mater. 191–194 (1992) 808.
[19] N. Hashimoto, E. Wakai, J.P. Robertson, J. Nucl. Mater. 273 (1999) 95.
[20] G.R. Odette, D. Frey, J. Nucl. Mater. 85&86 (1979) 817.
[21] C.W. Andrews, Met. Prog. 70 (7) (1950) 85.